their episodes of vertigo to a particular stress situation. In previous studies, stress in patients with Ménière's disease was evaluated by life events, psychological tests and behavioral characteristics [2, 4]. Recently, stress-related hormones have been widely measured for evaluation of stress [3, 5]. But hormonal responses to stress are intertwined with various factors and differ greatly between individuals. On that account, it is difficult to objectively assess the stress responses in patients with stress-related disorders including Ménière's disease.

Nowadays, microarray analysis is recognized as a useful clinical device for making diagnostic, therapeutic or prognostic decisions for several diseases [6, 7]. Further, psychological stress is known to stimulate the hypothalamic-pituitary-adrenal axis, sympathetic nervous system and immune system. These systems interact with each other, leading to complex stress responses [8, 9]. Analysis of gene expression by microarray may have a potential advantage of allowing to study complex responses, such as psychological stress, in which the measurement of a limited number of gene products does not always reflect the status of the disorders.

In our previous study, we developed a cDNA microarray specifically designed to measure mRNA levels of stress-related genes in peripheral blood leukocytes and have succeeded in identifying marker genes for assessment of acute psychological stress in healthy subjects [10]. In this study, to investigate the link between stress and vertigo attacks in Ménière's disease, we used the microarray and assessed the stress responses in patients with Ménière's disease by measuring the expression profiles of stress-related genes in peripheral blood leukocytes.

Subjects and Methods

We listed stress-related genes (stress hormones, neurotransmitters, cytokines, growth factors, receptors, signal transduction molecules, transcription factors, heat shock proteins, growth- or apoptosis-associated factors and metabolic enzymes) from the UniGene database of the National Center for Biotechnology Information. Target sequences of the listed genes were designed using original software (Hitachi, Saitama, Japan) and we selected 1,467 genes that were actually amplified by reverse transcriptase-PCR using total RNA isolated from peripheral leukocytes of healthy volunteers. The full list of genes can be seen at the following site: http://www.hitachi.co.jp/. All PCR products were sequenced to be the corresponding cDNAs, and they were spotted on the array according to the method previously described [11]. The microarray showed high reproducibility with a mean coefficient of variation of less than 20% and the dynamic ranges were three orders of magnitude. The expression of stress-related genes using this microarray has been described elsewhere [10].

Firstly, we examined the gene expression profiles in 2 female patients (43 and 44 years old) with definite Ménière's disease, diagnosed according to the guidelines for the diagnosis and evaluation of therapy in Ménière's disease [1]. Venous blood (10 ml) was then taken under fasting conditions from these patients during an attack, in the active phase and in the remission phase. We then compared the relative expression values of 782 genes during the attack or in the active phase with those in the remission phase. During the attack, patients developed a vertigo attack with spontaneous nystagmus. In the active phase, patients felt dizziness and showed a positional or positioning nystagmus around vertigo attacks. In the remission phase, patients had no vertigo, dizziness or nystagmus.

Next, 5 normal healthy volunteers (3 males and 2 females, ranging in age from 23 to 25 years) were recruited to examine the effects of caloric stimulation on stress-related gene expression profiles in peripheral blood leukocytes. These subjects had no history of neuro-otological or somatopsychic diseases and were taking no medication. Venous blood (10 ml) was collected under fasting conditions from each subject before and 2 h after caloric stimulation with 5 ml of ice-cold water for 20 s.

From each sample, 5 μg of total RNA were amplified using in vitro transcription reaction. The synthesized cDNA was labeled with dye (NHS-ester Cy5 or Cy3; Amersham Biosciences, Piscataway, N.J., USA) [12]. Cy5-cDNAs prepared from each sample were mixed with the equivalent amount of Cy3-cDNAs from the respective reference and the mixture was applied to the cDNA microarray. Signal intensities of Cy5 and Cy3 were quantified and analyzed by subtracting the backgrounds, using Quant Array software (GSI-Lumonics). The intensity values for duplicate cDNA probes were averaged. Following global normalization, we selected 782 genes with fluorescence intensity higher than the cutoff value of 300 in both conditions (labeled with Cy5 or Cy3) among 5 samples. The relative expression values for 782 genes (Cy5/Cy3) were subjected to hierarchical clustering using Gene Spring 6.0 software (Silicon Genetics, Redwood City, Calif., USA) and similarity analysis performed by standard correlation [13]. After that, Cy5/Cy3 ratios of 782 were transformed to logarithms. Because the coefficient of variation of this microarray is less than 20%, we judged that the gene expression was altered when its mRNA level was more than twofold or less than half of the control value.

The present study was approved by the Human Study Committee of Tokushima University Hospital and informed consent was obtained from each individual prior to the study.

Results

Figure 1 shows the hierarchical cluster analysis of the relative expression values of 782 stress-related genes in the attack and active phases in 2 patients with definite Ménière's disease over those in the remission phase. Accordingly, the relative expressions of the stress-related genes were uniformly up-regulated or down-regulated in the attack and active phases. Overall changes in 782 mRNA levels of stress-related genes of 2 patients with Ménière's disease in the attack and active phases are shown in figure 2. Patient 2 who had an intractable course

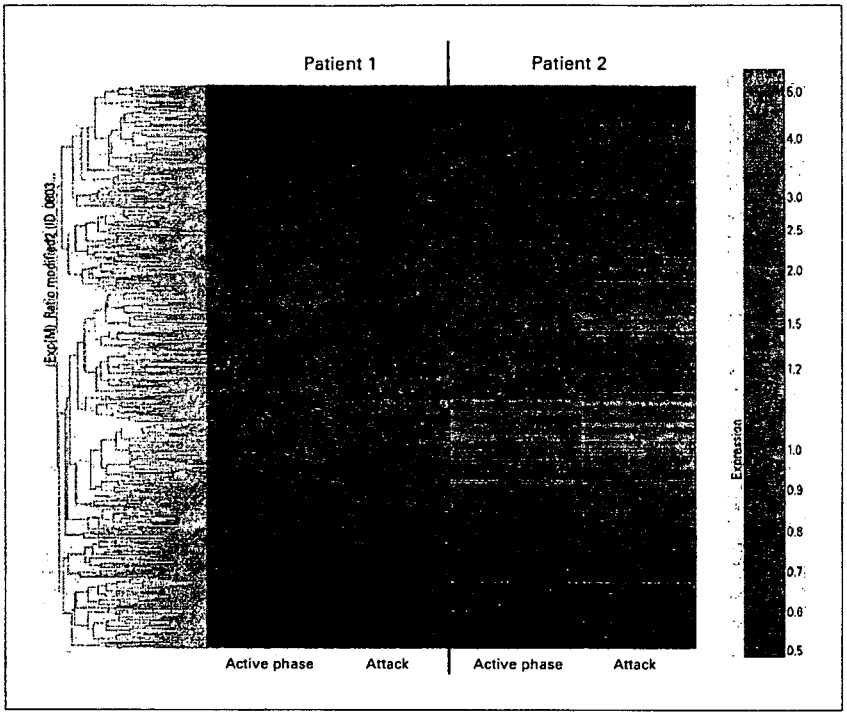

Fig. 1. Hierarchical clustering of psychological stress-related changes in relative gene expression in the attack and active phases in patients with Ménière's disease over those in the remission phase.

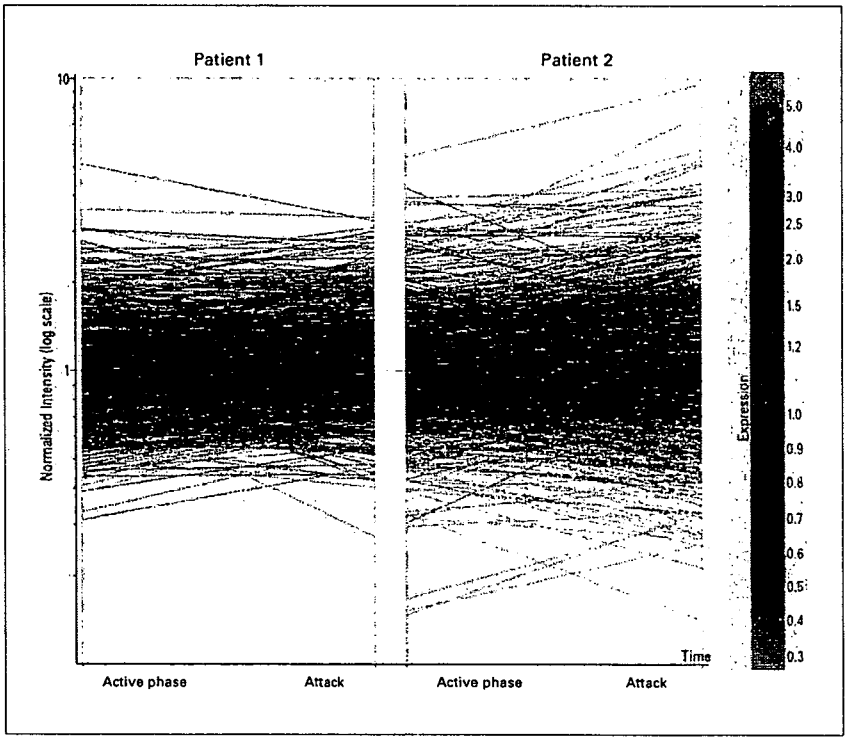

Fig. 2. Overall changes in the expression values of stress-related genes in patients with Ménière's disease in the attack and active phases.

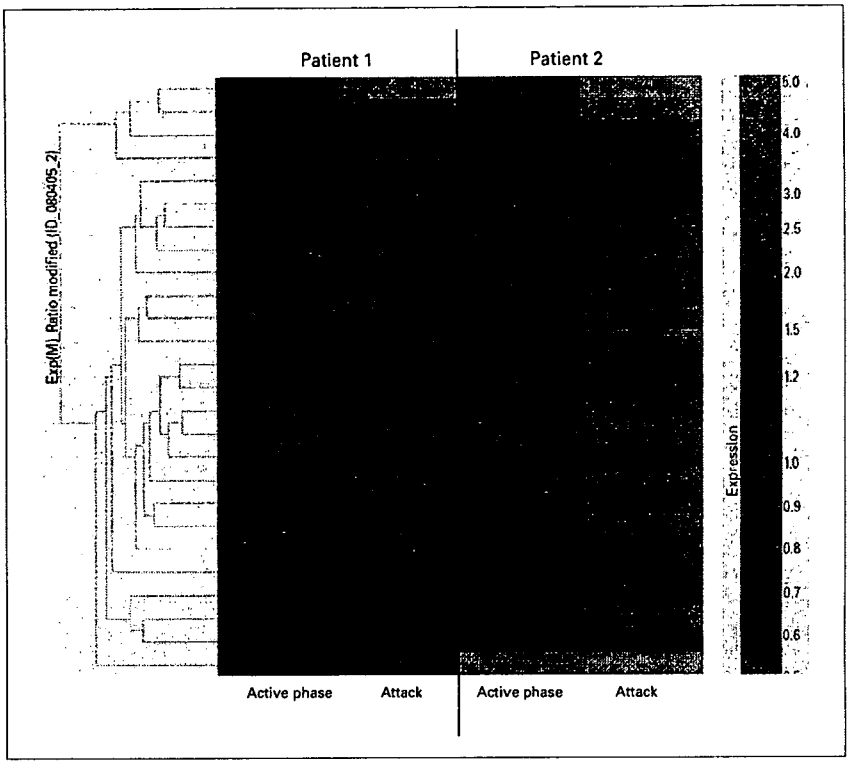

Fig. 3. Hierarchical clustering of 26 significantly responsive overlapping genes in the attack and active phases in 2 patients with Ménière's disease over those in the remission phase.

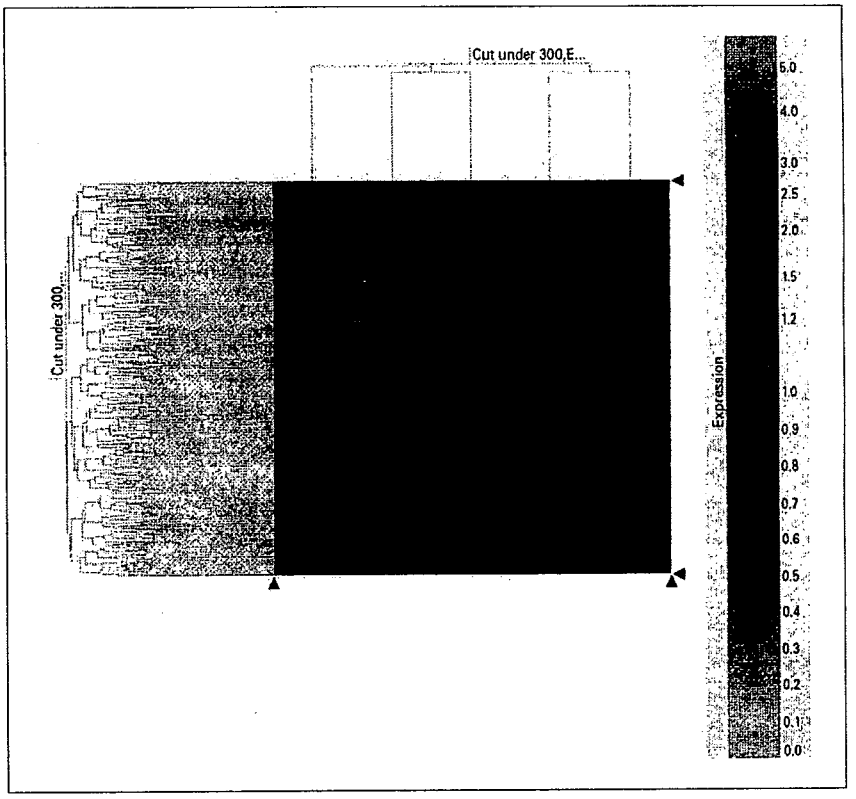

Fig. 4. Hierarchical clustering of psychological stress-related changes in relative gene expression pattern 2 h after caloric stimulation over the precaloric ones in 5 normal subjects.

with frequent vertigo attacks exhibited more profound changes in gene expression than patient 1, who had sporadic episodes of vertigo. Indeed, we identified 57 genes in patient 1 and 163 genes in patient 2, of which mRNA levels, respectively, increased over twofold or decreased by less than half in the attack and active phases in comparison with the remission phase. Twenty-six genes were then identified to commonly change in both patients in the attack and active phases. Figure 3 shows the hierarchical cluster analysis of the relative expression values of those commonly changing 26 genes in the attack and active phases in 2 patients with definite Ménière's disease over those in the remission phase. Most of these 26 genes were cytokine-related genes (data not shown).

Figure 4 shows the hierarchical cluster analysis of the relative expression values of 782 genes 2 h after the caloric stimulation with cold water over the precaloric ones in 5 normal subjects. All subjects showed caloric nystagmus with sensation of vertigo. However, the caloric stimulation changed none of the mRNA levels for 782 genes over twofold or less than half.

Discussion

In the present study, we showed that vertigo attacks in patients with definite Ménière's disease are accompanied by a marked change in stress-related gene expression in peripheral leukocytes (fig. 1, 2). It has been reported that stressful life events trigger vertigo attacks in Ménière's disease [2, 3]. Sawada et al. [14] reported that about three fourths of patients with Ménière's disease were aware of stressful events before an attack of vertigo. A time-series analysis also showed that the incidence of stress increased on the same day of vertigo onset in patients with Ménière's disease. Indeed, a recent report by Soderman et al. [15] stated that the risk of having an attack of Ménière's disease is increased during 3 h after being exposed to emotional stress.

At the same time, vertigo itself is known to cause anxiety and panic in Ménière's patients, which may induce stress responses. However, it is not likely, as demonstrated by our data, that changes in expression profiles of stress-related genes during the acute phases in patients with Ménière's disease are secondary to vertigo or vertigo-associated anxiety. In fact, the expression of stress-related genes did not significantly change after caloric stimulation, which caused acute vertigo with nystagmus in healthy volunteers (fig. 4).

In the attack and active phases, mRNA expression levels of 57 genes and 163 genes were either up-regulated more than twofold or down-regulated by less than half in patient 1 and patient 2, respectively (fig. 1). Moreover, the magnitude of changes in gene expression in patient 2 seemed to be larger than that in patient 1 (fig. 2). Patient 1 had sporadic episodes of vertigo, while patient 2 had an intractable course with frequent vertigo attacks, suggesting that the number of genes whose mRNA expressions were changed and the magnitude of their changes are correlated with the severity of the disorder. These findings suggest that protein products of stress-related genes, such as stress-related hormones, contribute to the development of vertigo attacks in Ménière's disease.

In addition, the hypothalamic-pituitary-adrenal (HPA) axis and the sympathetic nervous system have been known to play an essential role in stress responses [16]. Excessive, prolonged or inadequate stress response leads to pathological outcomes. In fact, stress response in patients with Ménière's disease has been evaluated by measuring concentrations of several stress-associated hormones such as epinephrine, vasopressin, aldosterone, growth hormone, prolactin, cortisol, adrenocorticotrophic hormone (ACTH) [3, 5, 14, 17]. It was reported that there exist a strong positive correlation between cortisol and ACTH in patients with Ménière's disease and a significant positive correlation between cortisol and prolactin in female patients with Ménière's disease. It was suggested that patients with Ménière's disease are in a state of chronic stress where the PHA axis is perturbed [5]. Although dysregulation of HPA axis activity may be involved in the pathogenesis of Ménière's disease, especially endolymphatic hydrops, it is difficult to use stress-related hormones to adequately assess the stress response that is regulated by the complex brain-immune-endocrine networks. High-throughput analysis of gene expression by microarray has a potential advantage in clarifying the complex stress-related responses.

Our unique cDNA microarray specifically designed to assess stress responses in peripheral blood leukocytes identified 26 stress-related genes that commonly changed in both patients (fig. 3). As patient 2 showed more pronounced changes in mRNA expression of more than half of the 26 genes, changes in the expression of these 26 genes appeared to be parallel to the severity of Ménière's disease. Most of these genes are classified into inflammation-related molecules. It is suggested that this distinct group of stress-related genes contributes to the development of vertigo attacks in Ménière's disease. The present analysis, limited to only 2 patients with Ménière's dis-

ease, is not entirely conclusive, but our ongoing study with a larger number of patients will give us more insight into how these genes interact to trigger vertigo attacks in Ménière's disease. Finally, stress-related gene expression profiles in peripheral leukocytes may be a predictive and therapeutic tool for episodic vertigo attacks in patients with Ménière's disease.

Acknowledgment

This study was supported by grants for studies on vestibular disorders financed by the Japanese Ministry of Health and Welfare.

References

1 Committee on Hearing and Equilibrium: Guidelines for the diagnosis and evaluation of therapy in Ménière's disease. Otolaryngol Head Neck Surg 1995;113:181–185.

2 Andersson G, Hagnebo C, Yardley L: Stress and symptoms of Ménière's disease: a time-series analysis. J Psychosom Res 1997;43:595–603.

3 Horner KC, Cazals Y: Stress in hearing and balance in Ménière's disease. Noise Health 2003;5:29–34.

4 Takahashi M, Ishida K, Iida M, Yamashita H, Sugawara K: Analysis of lifestyle and behavioral characteristics in Ménière's disease patients and a control population. Acta Otolaryngol 2001;121:254–256.

5 Horner KC, Cazals Y: Stress hormones in Ménière's disease and acoustic neuroma. Brain Res Bull 2005;66:1–8.

6 Bullinger L, Döhner K, Bair E, Fröhling S, Schlenk RF, Tibshirani R, Döhner H, Pollack JR: Use of gene-expression profiling to identify prognostic subclasses in adult acute myeloid leukemia. N Engl J Med 2004;350:1605–1616.

7 Van De Vijver MJ, He YD, Van't Veer LJ, Dai H, Hart AAM, Voskuil DW, Schreiber GJ, Peterse JL, Roberts C, Marton MJ, Parrish M, Atsma D, Witteveen A, Glas A, Delahaye L, Van Der Verde T, Bartelink H, Rodenhuis S, Rutgers ET, Friend SH, Bernards R: A gene-expression signature as a predictor of survival in breast cancer. N Engl J Med 2002;347:1999–2009.

8 Connor TJ, Leonard BE: Depression, stress and immunological activation: the role of cytokines in depressive disorders. Life Sci 1998;62:583–606.

9 Raison CL, Miller AH: When not enough is too much: the role of insufficient glucocorticoid signaling in the pathophysiology of stress-related disorders. Am J Psychiatry 2003;160:1554–1565.

10 Morita K, Saito T, Ohta M, Ohmori T, Kawai K, Teshima-Kondo S, Rokutan K: Expression analysis of psychological stress-associated genes in peripheral blood leukocytes. Neurosci Lett 2005;381:57–62.

11 Schena M, Shalon D, Davis RW, Brown PO: Quantitative monitoring of gene expression patterns with a complementary DNA microarray. Science 1995;270:467–470.

12 Hughes TR, Mao M, Jones AR, Burchard J, Marton MJ, Shannon KW, Lefkowitz SM, Ziman M, Schelter JM, Meyer MR, Kobayashi S, Davis C, Dai H, He YD, Stephaniants SB, Cavet G, Walker WL, West A, Coffey E, Shoemaker DD, Stoughton R, Blanchard AP, Friend SH, Linsley PS: Expression profiling using microarrays fabricated by an ink-jet oligonucleotide synthesizer. Nat Biotechnol 2001;19:342–347.

13 Long AD, Mangalam HJ, Chan BY, Tolleri L, Hatfield GW, Baldi P: Improved statistical inference from DNA microarray data using analysis of variance and a Bayesian statistical framework: analysis of global gene expression in *Escherichia coli* K12. J Biol Chem 2001;276:19937–19944.

14 Sawada S, Takeda T, Saito H: Antidiuretic hormone and psychosomatic aspects in Ménière's disease. Acta Otolaryngol Suppl 1997;528:109–112.

15 Soderman AC, Moller J, Bagger-Sjoback D, Bergenius J, Hallqvist J: Stress as a trigger of attacks in Ménière's disease: a case-crossover study. Laryngoscope 2004;114:1843–1848.

16 Scott LV, Dinan TG: Vasopressin and the regulation of hypothalamic-pituitary-adrenal axis function: implications for the pathophysiology of depression. Life Sci 1998;62:1985–1998.

17 Juhn SK, Li W, Kim JY, Javel E, Levine S, Odland RM: Effect of stress-related hormones on inner ear fluid homeostasis and function. Am J Otol 1999;20:800–806.

Available online at www.sciencedirect.com
SCIENCE DIRECT
Neuroscience Letters 379 (2005) 23–26
Neuroscience Letters
www.elsevier.com/locate/neulet

Effects of immersion in virtual reality on postural control

Hironori Akizuki[a], Atsuhiko Uno[b], Kouichi Arai[c,1], Soukichi Morioka[d], Seizo Ohyama[a], Suetaka Nishiike[b], Koichi Tamura[a], Noriaki Takeda[a,*]

[a] *Department of Otolaryngology, University of Tokushima School of Medicine, 3-18-15 Kuramoto, Tokushima 770-0042, Japan*
[b] *Department of Otolaryngology and Sensory Organ Surgery, Osaka University Graduate School of Medicine, Osaka 565-0871, Japan*
[c] *General Research and Development Center, Kansai Electric Power Co. Ins., Hyogo 661-0974, Japan*
[d] *Laboratories of Image Information Science and Technology, Osaka 559-0034, Japan*

Received 22 June 2004; received in revised form 14 September 2004; accepted 18 December 2004

Abstract

In the present study, we examined the effects of the time lag between visual scene and the head movement in the virtual reality (VR) world on motion sickness and postural control in healthy volunteers. After immersion in VR with additional time lags (from 0 to 0.8 s) to the inherent delay (about 250 ms), the visual-vestibular conflict induced a slight motion sickness in experimental subjects, but no change was noticed in the body sway path with eyes open and closed. However, Romberg ratio of body sway path with eyes closed divided by that with eyes open after immersion in VR was significantly decreased in comparison with that before immersion in VR. Since Romberg ratio is an index of visual dependency on postural control, this finding indicates that the immersion in VR decreases the visual dependency on postural control. It is suggested that adaptation to visual-vestibular conflict in VR immersion increases the contribution of vestibular and somatosensory inputs to postural control by ignoring the conflicting delayed visual input in the VR world. VR may be a promising treatment for visual vertigo in vestibular patients with unsuccessful compensation by its ability to induce vestibular and somatosensory reweighing for postural control.

Keywords: Virtual reality; Motion sickness; Body sway path; Romberg ratio; Visual vertigo

Computer graphics technology called virtual reality (VR) creates a visual scene, in which the user feels immersed. As the user makes active head movements, the computer determines the new direction of gaze and recreates the scene from the new point of view. In the VR world, the visual scene is delayed after the head movement by about several hundreds milliseconds. Therefore, the interaction between active head movements and the display of the VR scene is different from the same interaction in the real world. In VR, this interaction results in a visual-vestibular conflict (VVC) which prompts the user to adapt to the newly displayed scene. In this process of the adaptation, some users may develop motion sickness and show postural disequilibrium [10,13].

In our previous study, we created the VR world in Cave Automatic Virtual environment (CAVE, Electronic Visualization Laboratory, University of Illinois, Chicago, USA) to induce a twofold visual-vestibular discrepancy for angular head movement, and reported that the VVC in the VR world induced motion sickness and postural instability in humans [1].

In the present study, we used a head mounted display (HMD) and examined the effects of additional time lags to the inherent delay of the visual scene after head movement in the VR world on subjective motion sickness scores and postural control measured by platform posturography.

Subjects were 23 healthy young male volunteers (mean age: 21.9 years old). They were previously informed about the VR system and the details of the experiment. Subjects were also warned of a possible interruption of the experiment when their discomfort or ataxia should become serious. After obtaining the volunteers' informed consent, the exper-

* Corresponding author. Tel.: +81 88 633 7169; fax: +81 88 633 7170.
E-mail address: takeda@clin.med.tokushima-u.ac.jp (N. Takeda).
[1] Present address: Office of Corporate Auditors, Kansai Electric Power Co. Ins., Hyogo 661-0974, Japan.

0304-3940/$ – see front matter © 2004 Elsevier Ireland Ltd. All rights reserved.
doi:10.1016/j.neulet.2004.12.041

iment was conducted in accordance with the Declaration of Helsinki.

The levels of severity of motion sickness were estimated as numerical scores according to Graybiel's criteria: a multi-symptom checklist to assess motion sickness symptomatology [9]. Higher scores of the questionnaire reflect more severe symptoms.

Body sway was recorded with a force platform (GS-30, Anima, Japan) under both conditions: with eyes open and closed. The length of body sway path traveled for 60 s was measured and the Romberg ratio was calculated as the value with eyes closed divided by that with eyes open.

The VR system used in the present study was developed by Kansai Electric Power Co. Inc. as a tool for training inspectors of a high voltage transformer substation. Accordingly, subjects wore HMD (HMD STV-E, Shimizu, Japan) that presents two images individually to each eye for stereoscopy. Their head movements were monitored by magnetic sensors (Fastrak, Phemus, USA) equipped with head gear. During active head movement, the graphic workstation (ONYX RE2, SilliconGraphics, USA) provided the new direction of gaze and the scene from the new point of view through HMD. The visual scene is usually delayed after the head movement by about 250 ms. Subjects wore the Cyber Touch without vibrotactile function (Virtual Technologies, USA) of their right hand that monitored the position and angle of the hand and figures, when subject used his hand in the VR world. During immersion in the VR, subjects were asked to move and complete steps of inspection with their right hand, such as opening the door, turning on/off the button, etc., following examiner's instructions.

The first experiment was performed under the following conditions: (1) without HMD, (2) with transparent HMD but not immersed in VR and (3) with HMD and immersed in VR. The subjects were instructed to stand upright with their feet together on a platform with eyes open while their body sway was recorded for 60 s.

In the second experiment, before immersion in VR (PRE), subjects without HMD were instructed to stand in the same position while their body sway was recorded with both eyes open and closed for 60 s, respectively. Next, subjects were immersed in VR for 15 min. After the first period of the VR immersion (1ST), the body sway and motion sickness scores were also recorded under the same conditions. Finally, after eight times immersion in the VR for 3 min at 5 min intervals (POST), the body sway and motion sickness scores were also recorded. In each VR immersion for 3 min, additional time lag to the inherent delay of the visual scene that the computer recreates behind the head movement was applied. The duration of additional time lag randomly varied between 0, 0.2, 0.4 and 0.8 s two times and was constant within each 3 min period of immersion.

These experiments were a part of the study to examine physiological and psychological effects of immersion in virtual reality in humans. Since the study was supported by Kansai Electric Power Co. Ins., the experimental design had been decided by its General Research and Development Center.

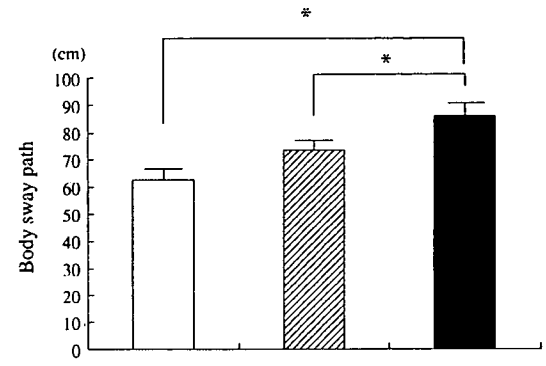

Fig. 1. Effects of wearing HMD and immersion in VR on body sway path. The open column shows the body sway path recorded for 60 s with eyes open without HMD. Hatched column: with HMD but not immersed in VR. Solid column: with HMD during immersion in VR. Columns and bars represent means ± S.E. ($n = 23$). $^*p < 0.05$.

Analysis of variance (ANOVA) with repeated measures followed by the post hoc Schefe test was used. Value of $p < 0.05$ was considered significant.

The body sway path increased in the following order: without HMD, with transparent HMD but not immersed in VR and with HMD and immersed in VR (Fig. 1). The body sway path with HMD during immersion in VR was significantly increased in comparison with that without HMD and that with transparent HMD but not immersed in VR.

Immersion in VR did not induce frank motion sickness in any subjects. After completing steps of inspection with the right hand in the VR world with additional time lag, subjects developed a slight motion sickness (Table 1). Motion sickness scores according to Graybiel's criteria were 1.8 ± 0.4 (mean ± S.E.) after 1ST and 1.6 ± 0.4 after POST. The present study includes eight times immersion in VR for 3 min at 5 min intervals with additional time lags varying from 0 to 0.8 s and examined the effects of duration of time lags of visual scene after the head movement on motion sickness. The scores of Graybiel's criteria were estimated eight times after each VR immersion for 3 min. However, all time lags did not induce apparent motion sickness (data not shown).

After completing the steps of inspection with the right hand in the VR world with additional time lag, no postural instability was induced. The body sway path with eyes open was 62.9 ± 3.5 cm at PRE, 64.0 ± 3.4 cm after 1ST, 64.2 ± 2.8 cm after POST (Fig. 2a), and that with eyes

Table 1
Changes in motion sickness score

Levels of severity (points)	PRE	1ST	POST
Frank sickness (>16)	0	0	0
Severe malaise (15–8)	0	0	0
Moderate malaise A (7–5)	0	3	3
Moderate malaise B (4–3)	0	4	4
Slight malaise (2–1)	0	7	6
No malaise (0)	23	9	10

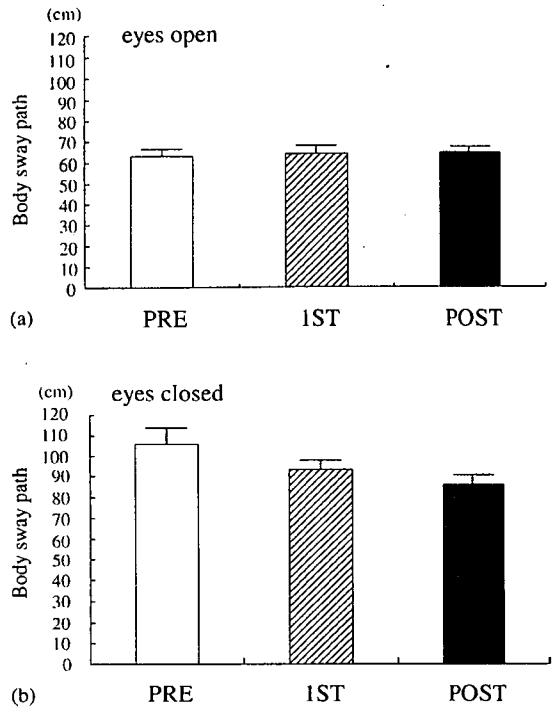

Fig. 2. (a and b) Effects of immersion in VR on body sway path. Body sway path was recorded for 60 s with eyes open (a) and closed (b). Open column: without HMD before immersion in VR (PRE). Hatched column: after taking off HMD, body sway path was recorded after the first immersion in VR for 15 min (1ST). Solid column: after taking off HMD, body sway path was recorded after eight times immersion in VR with additional time lags for 3 min at 5 min intervals (POST). Columns and bars represent mean ± S.E. ($n = 23$). $^*p < 0.05$.

closed was 105.6 ± 7.8 cm at PRE, 93.2 ± 4.7 cm after 1ST, 86.1 ± 4.5 cm after POST (Fig. 2b). Thus, the body sway path with eyes open and closed did not change neither after the first immersion in VR for 15 min or after eight times VR immersion with additional time lag to the inherent delay for 3 min at 5 min intervals. However, the Romberg ratio of body sway path with eyes closed divided by that with eyes open was 1.7 ± 0.1 at PRE, 1.5 ± 0.1 after 1ST and 1.3 ± 0.1 after POST (Fig. 3). Thus, after the first and the last immersion in VR, the Romberg ratio was significantly decreased in comparison with that before immersion in VR.

The neural mismatch hypothesis of motion sickness that conflicting inputs from visual, vestibular and somatosensory systems produce motion sickness is widely accepted [11,12,14]. Because the visual scene in VR system is delayed after the head movement by about several hundred milliseconds, it was reported that the new visual-vestibular interaction in the VR world developed motion sickness and postural instability in VR user [10,13]. In the present study, subjects with HMD developed a slight motion sickness after the first VR immersion. However, subsequent VR immersion with additional time lags behind head movement to the inherent delay did not induce build-up of motion sickness symptoms (Table 1). This finding was not consistent with our previous

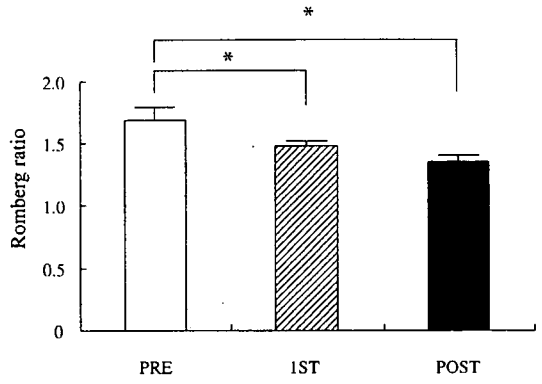

Fig. 3. Effects of immersion in VR on Romberg ratio of body sway path. Open column: Romberg ratio of PRE. Hatched column: Romberg ratio of 1ST. Solid column: Romberg ratio of POST. Columns and bars represent mean ± S.E. ($n = 23$). $^*p < 0.05$.

finding that the twofold VVC in the VR world of CAVE induced gradual development of motion sickness [1]. There are three possible reasons why the VVC in the VR world with time discrepancy up to 0.8 s between the visual scene and the head movement did not induce motion sickness. The first is that the degree of VVC with additional time lags was smaller than that of the twofold VVC in CAVE and was not enough to develop motion sickness. The second is that visual-visual discrepancy in CAVE between small visual clues of the real world and delayed visual input of VR does not exist with HMD. The third is that adaptation to VVS with additional time lags developed so quickly that motion sickness did not manifest. The last explanation is likely in that it is in line with the report that repeated exposure to provocative motion like the present procedure was effective in developing adaptation as compared to exposure to a prolonged provocative motion [8].

In the present study, the body sway path during immersion in VR with HMD was significantly increased (Fig. 1). However, after completing steps of inspection with the right hand in the VR world and taking off the HMD, postural instability was not induced. The body sway path with eyes open and closed changed neither after the first immersion in VR for 15 min nor after eight times VR immersion with additional time lags up to 0.8 s for 3 min at 5 min intervals (Fig. 2). These findings were not in line with our previous findings in CAVE that demonstrated an increase in the area of body sway with both eyes open and closed immediately after the immersion in VR [1]. However, in the present study, the Romberg ratio of the body sway path was significantly decreased after immersion in VR with additional time lags (Fig. 3). The Romberg ratio calculated as the value of the body sway path with eye closed divided by that with eyes open, was an index of visual dependency on posture control. Therefore, the present finding suggests that adaptation to the VVC in VR immersion decreases the visual dependency on posture control. In fact, it has been reported that postural control adapts to different environments by integrating visual, vestibular and so-

matosensory inputs and by changing the contribution of each to fit the circumstance [2,7]. Other reports have suggests that when the information relayed by the visual system becomes inappropriate or unreliable, the relative weight of the visual dependency on postural control decreases immediately [3,4]. Consequently, the present finding suggests that in the process of adaptation to the VVC in VR immersion, the contribution of vestibular and somatosensory inputs to postural control increases by ignoring the conflicting delayed visual input in the VR world.

Visual vertigo symptoms are common in vestibular patients with unsuccessful compensation. These patients feel dizzy in visual surroundings such as supermarket aisle, unstable visual backgrounds (traffic, crowds, and moving objects) and in certain driving conditions [5]. This observation was confirmed by the report that patients with visual vertigo showed high visual field dependency [6]. However, the most effective rehabilitation method for visual vertigo remains an open question. Since the present findings suggest that adaptation to certain VR environments decreases the contribution of visual inputs to postural control, VR may be a promising treatment for visual vertigo by its ability to reweigh vestibular and somatosensory inputs for postural control.

Acknowledgment

This study was supported by a Health Science Research Grant for Specific Disease from the Ministry for Health and Welfare, Japan and Grant-in-Aid for Scientific Research from the Japan Society for the Promotion of Science.

References

[1] H. Akizuki, S. Nishiike, H. Watanabe, K. Matsuoka, T. Kubo, N. Takeda, Visual-vestibular conflict induced by virtual reality in humans, Neurosci. Lett. 340 (2003) 197–200.
[2] A. Berthoz, B. Pavard, L.R. Young, Perception of linear horizontal self-rotation induced by peripheral vision (linearvection) basic characteristics and visual-vestibular interaction, Exp. Brain Res. 23 (1975) 471–489.
[3] A.M. Bronstein, Suppression of visually evoked postural responses, Exp. Brain Res. 63 (1986) 655–658.
[4] A.M. Bronstein, Visual control of balance in cerebellar and Parkinsonism syndromes, Brain 13 (1990) 767–779.
[5] A.M. Bronstein, The visual vertigo syndrome, Acta Otolaryngol. Suppl. 520 (1995) 45–48.
[6] A.M. Bronstein, Visual vertigo syndrome: clinical and posturography findings, J. Neurol. Neurosurg. Psychiatry 59 (1995) 472–476.
[7] J. Dichgans, T. Brandt, Optokinetic motion sickness and pseudoeffects induced by moving visual stimuli, Acta Otolaryngol. 76 (1973) 339–348.
[8] J.F. Golding, J.R.R. Stott, Effect of sickness severity on habituation to repeated motion sickness challenges in aircrew referred for airsickness treatment, Aviat. Space Environ. Med. 66 (1995) 625–630.
[9] A. Graybiel, C.D. Wood, E.F. Miller, D.B. Cramer, Diagnostic criteria for grading the severity of acute motion sickness, Aviat. Space Environ. Med. 39 (1968) 453–455.
[10] E.M. Kolasinski, R.D. Gilson, Ataxia following exposure to a virtual environment, Aviat. Space Environ. Med. 70 (1999) 264–269.
[11] C.M. Oman, Motion sickness: a synthesis and evaluation of the sensory conflict theory, Can. J. Physiol. Pharmacol. 68 (1990) 294–303.
[12] J.T. Reason, Motion sickness adaptation: a neural mismatch model, J. R. Soc. Med. 71 (1978) 819–829.
[13] E.C. Regan, K.R. Price, The frequency of occurrence and severity of side-effects of immersion virtual reality, Aviat. Space Environ. Med. 65 (1994) 527–530.
[14] N. Takeda, M. Morita, A. Horii, S. Nishiike, T. Kitahara, A. Uno, Neural mechanisms of motion sickness, J. Med. Invest. 48 (2001) 44–59.

Available online at www.sciencedirect.com
SCIENCE DIRECT
Brain Research 1063 (2005) 96 – 101
BRAIN RESEARCH
www.elsevier.com/locate/brainres

Research Report

Regional difference in corticotropin-releasing factor immunoreactivity in mossy fiber terminals innervating calretinin-immunoreactive unipolar brush cells in vestibulocerebellum of rolling mouse Nagoya

Masahiro Ando[a], Kazuhiko Sawada[b,*], Hiromi Sakata-Haga[b], Young-Gil Jeong[c], Noriaki Takeda[a], Yoshihiro Fukui[b]

[a]*Department of Otolaryngology, University of Tokushima Graduate School Institute of Health Biosciences, Tokushima 770-8503, Japan*
[b]*Department of Anatomy and Developmental Neurobiology, University of Tokushima Graduate School Institute of Health Biosciences, Tokushima 770-8503, Japan*
[c]*Department of Anatomy, College of Medicine, Konyang University, Nonsan, Chungnam, South Korea*

Accepted 25 September 2005
Available online 27 October 2005

Abstract

Unipolar brush cells (UBCs), a class of interneurons in the vestibulocerebellum, play roles in amplifying excitatory inputs from vestibulocerebellar mossy fibers. This study aimed to clarify whether corticotropin-releasing factor (CRF)-positive mossy fiber innervation of calretinin (CR)-positive UBCs was altered in rolling mouse Nagoya (RMN). The distribution and the number of CR-positive UBCs in the vestibulocerebellum were not different between RMN and control mice. Double immunofluorescence revealed that some CRF-positive mossy fiber terminals were in close apposition to CR-positive UBCs. In the lobule X of vermis, such mossy fiber terminals were about 5-fold greater in number in RMN than in controls. In contrast, the number of CRF-positive mossy fiber terminals adjoining CR-positive UBCs in the flocculus was not significantly different between RMN and controls. The results suggest increased number of CRF-positive mossy fiber terminals innervating CR-positive UBCs in the lobule X but not in the flocculus of RMN. CRF may alter CR-positive UBC-mediated excitatory pathways in the lobule X of RMN and may disturb functions of the lobule X such as cerebellar adaptation for linear motion of the head.

Theme: Disorders of the nervous system
Topic: Genetic models

Keywords: Rolling mouse Nagoya; Ataxia; Corticotropin-releasing factor; Unipolar brush cell; Mossy fiber; Vestibulocerebellum

1. Introduction

Rolling mouse Nagoya (RMN) is a hereditary ataxic mutant mouse first described by Oda [15] and characterized by a severe ataxic gait and abnormal hindlimb extension [25]. RMN carries a mutation in a recessive autosomal allele of the *tottering* locus on chromosome 8 [16] that encodes a gene for α_{1A} subunit of P/Q-type Ca^{2+} channel ($Ca_V2.1$) [11] as do *tottering*, *leaner* [9] and *rocker* mice [27]. In humans, defects in this gene are responsible for several neurological disorders such as episodic ataxia type-2 (EA-2) and familial hemiplegic migraine [17]. In recent studies of the cerebellum of RMN, strong α_{1A} subunit immunostaining appears in Purkinje cells [21], and the voltage sensitivity and activity of the P/Q-type Ca^{2+} channel are selectively reduced in those neurons [11]. We have also reported an increased expression of tyrosine hydroxylase in particular subsets of Purkinje cells of the cerebellum of RMN [18–20] without activation of this enzyme [23].

* Corresponding author. Fax: +81 88 633 7053.
E-mail address: sawada@basic.med.tokushima-u.ac.jp (K. Sawada).

0006-8993/$ - see front matter © 2005 Elsevier B.V. All rights reserved.
doi:10.1016/j.brainres.2005.09.018

Unipolar brush cells (UBCs), a class of interneurons in the granule cell layer of the cerebellum, have been reported in the mouse, rat and other mammalian species [4,6,12]. UBCs receive excitatory inputs from the primary and secondary vestibulocerebellar mossy fibers (extrinsic mossy fibers) and give rise to axons (intrinsic mossy fibers) which innervate granule cells and other UBCs [8,13]. Thus, UBCs form excitatory feedforward pathways within the basic cerebellar circuits and play an important role in cerebellar control for equilibrium. Recent studies have reported the presence of two distinct subsets of UBCs in the vestibulocerebellum, i.e., calretinin (CR)-positive and mGluR1α-positive UBCs [14]. These two UBC subsets are generated from distinctly different origins [24] and supposed to organize non-overlapped different microcircuits in the cerebellum [14]. In some mammalian species, CR-positive UBCs are preferentially distributed in the cerebellar lobules associated with the vestibulo-ocular reflex [6]. Since human patients with EA-2 impaired otolith-mediated linear vestibulo-ocular reflex [26], altered modulation of CR-positive UBCs may be involved in this clinical symptom of Ca^{2+} channelopathy.

Corticotropin-releasing factor (CRF) serves as a neuromodulator to enhance glutamate sensitivity in the cerebellar circuits [2,3]. Our previous study revealed an increased CRF immunostaining in particular subsets of mossy fiber terminals in both the vestibulocerebellum and non-vestibular vermal lobules of RMN [22]. This study aimed to clarify whether CRF-positive mossy fiber innervation of CR-positive UBCs was altered in RMN. We examined double immunofluorescence for CR and CRF in the vestibulocerebellum of RMN and quantitatively evaluated the number of CRF-positive mossy fiber terminals adjoining CR-positive UBCs.

2. Materials and methods

2.1. Animals

Homozygous rolling mice (C3Hf/Na:tg^{rol}/tg^{rol}; RMN) raised by intercrossing between heterozygous pairs were easily identifiable by their ataxic locomotion between postnatal days 10 and 14. Wild-type mice (C3Hf/Na:+/+) were used as controls. Mice were given a pellet diet (NMF, Oriental Yeast Co., Ltd., Japan) and tap water ad libitum and were kept at 24 ± 1°C under 12-h artificial illumination. All animal procedures were done according to the *Guide for the Care and Use of Laboratory Animals* and were reviewed by the Institutional Animal Care and Use Committee of the University of Tokushima. Every effort was made to minimize the number of animals used and their suffering.

2.2. Tissue preparation

Male RMN (n = 8) and male control mice (n = 8) at 8 months were deeply anesthetized with an intraperitoneal injection of sodium pentobarbital (25 μg/10 g body weight) and were perfused with 10 ml of 0.9% NaCl followed by 100 ml of Bouin's solution without acetic acid at room temperature. Cerebella were immersed in the same fixative, embedded in paraffin and serially sectioned in the coronal plane at 3 μm. Deparaffinized sections were irradiated with microwaves for 5 min in 10 mM citrate buffer, pH 6.0, and processed for immunohistochemistry.

2.3. CR immunostaining

Sections were reacted with the rabbit anti-CR antiserum (1:20,000, Swant, Switzerland) containing 10% normal goat serum at 4°C overnight. After incubation, sections were rinsed with PBS and reacted with biotinylated goat anti-rabbit IgG. The immunoreactive products were visualized by Vectastain ABC elite kit (Vector Lab., Inc. Burlingame, CA, USA) using 0.01% 3,3′-diaminobenzidine tetrachloride in 0.03% H_2O_2 as a chromogen. The sections were counterstained with hematoxylin. Areas of the granule cell layer in the lobule X and flocculus were measured by Scion Image software (Scion Corporation, Frederick, MD, USA) on captured images, and the number of CR-positive UBCs was counted in those areas. Data were expressed as the number of CR-immunoreactive UBCs per mm^2 of granule cell layer.

2.4. Double immunofluorescence for CR and CRF

Sections were reacted with a mixture of the rabbit anti-CR antibody and the guinea pig anti-CRF antiserum (1:5,000, Peninsula Lab. Inc., CA, USA) containing 10% normal goat serum at 4°C overnight. After washing with PBS, sections were reacted with FITC-conjugated goat anti-rabbit IgG (1:200, MBL Co., Ltd., Nagoya, Japan) and Cy3-conjugated donkey anti-guinea pig anti-serum (1:200, Chemicon, Temecula, CA, USA). Images of double-immunostained sections were acquired with a confocal fluorescence microscope (Leica TCS-NT mounted on a Leica DMRB light microscope; Leica, Mannheim, Germany). Areas of the granule cell layer of the lobule X and flocculus were measured by Scion Image software (Scion Corporation, Frederick, MD, USA) on captured images. Since the diameter of mossy fiber terminal is 2–12 μm [1], the number of CRF-immunoreactive profiles at 2–12 μm in diameter was counted as CRF-positive mossy fiber terminals within the granule cell layers of the lobule X and flocculus. Then, the number of CRF-positive mossy fibers adjoining CR-positive UBCs was also counted. These numbers were totaled for two sections spaced more than 30 μm apart. Data were expressed as the number of CRF-positive mossy fibers and the number of CRF-positive mossy fibers adjoining CR-positive mossy fibers per mm^2 of granule cell layer.

2.5. Statistical analysis

Quantitative data were statistically analyzed by two-way analysis of variance (ANOVA) with group (RMN and

control mice) and region (the lobule X and flocculus) as factors. Subsequently, contrast tests based on two-way ANOVA were performed for comparison between RMN and control mice.

3. Results

3.1. Distribution and number of CR-positive UBCs

CR-positive UBCs were preferentially distributed in the granule cell layer of the vestibulocerebellum, i.e., the ventral part of lobule IX, the lobule X (Figs. 1A, B), the flocculus and the ventral part of paraflocculus (Figs. 1C, D). The distribution of CR-positive UBCs was not different between RMN and the controls. The number of CR-positive UBCs per mm^2 of the granule cell layer was estimated in the lobule X and flocculus. Two-way ANOVA revealed no significant effect on either group ($F_{1,28}$ = 1.57, P = 0.220), region ($F_{1,28}$ = 2.20, P = 0.149) or group × region interaction ($F_{1,28}$ = 0.38, P = 0.542) (Table 1).

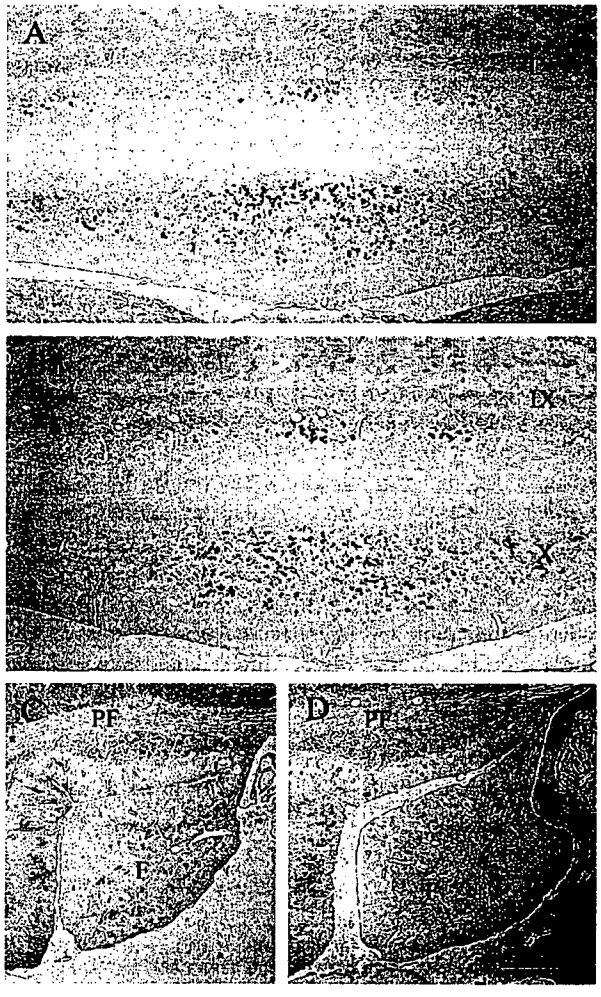

Fig. 1. Calretinin (CR) immunostaining in coronal sections of vermal lobules IX and X (A, B), flocculus and paraflocculus (C, D) of the cerebellum of a rolling mouse Nagoya (RMN) (A, C) and a control mouse (B, D). CR-positive UBCs were distributed in the granule cell layer of the ventral part of lobule IX, the lobule X, flocculus (F) and ventral part of the paraflocculus (PF). There was no difference in distribution of CR-positive UBCs between RMN and controls. Scale bar = 100 μm.

Table 1
Number of calretinin (CR)-positive UBCs per mm^2 of the granule cell layer in the vermal lobule X and flocculus of cerebellum (mean ± SEM)

Groups	n	Lobule X	Flocculus
RMN	8	95 ± 6.4	103 ± 16.8
Control	8	105 ± 8.1	130 ± 16.4

No significant effects on group ($F_{1,28}$ = 1.57, P = 0.220), region ($F_{1,28}$ = 2.20, P = 0.149) and group × region interaction ($F_{1,28}$ = 0.38, P = 0.542) (two-way ANOVA).

3.2. Double immunofluorescence for CR and CRF

Double immunofluorescence for CR and CRF was performed in the lobule X and flocculus. CRF-positive mossy fiber terminals were numerously found in the lobule X of RMN but a few in that of controls (Figs. 2A, B). Some CRF-positive mossy fibers were in close apposition to CR-positive UBCs (Figs. 2A, B). CRF-positive mossy fiber terminals were also found in the flocculus, but their number did not seem different between RMN and controls from visual evaluation (Figs. 2C, D). Like the lobule X, some CRF-positive mossy fiber terminals were in close apposition to CR-positive UBCs in the flocculus (Fig. 2C, D).

The number of CRF-positive mossy fiber terminals per mm^2 of the granule cell layer was estimated in the lobule X and flocculus, and the results are shown in Table 2. Two-way ANOVA revealed significant effects on either group ($F_{1,28}$ = 18.67, P < 0.001), region ($F_{1,28}$ = 13.22, P < 0.002) or group × region interaction ($F_{1,28}$ = 5.15, P < 0.05) (Table 2). The contrast tests detected a significant difference between RMN and the controls in the lobule X (P < 0.001). About a 2.5-fold greater number of CRF-positive mossy fibers was observed in RMN when compared to controls. In contrast, the number of those fiber terminals in the flocculus was not significantly different between RMN and controls.

The number of CRF-positive mossy fiber terminals adjoining CR-positive UBCs per mm^2 of the granule cell layer was further estimated in both the lobule X and flocculus. Two-way ANOVA showed significant effects on either group ($F_{1,28}$ = 9.16, P < 0.01), region ($F_{1,28}$ = 10.71, P < 0.005) or group × region interaction ($F_{1,28}$ = 7.14 P < 0.05) (Table 3). Intriguingly, the number of CRF-positive mossy fiber terminals adjoining CR-positive UBCs was about 5-fold greater in RMN than in the controls (P < 0.001) (Table 3). Just as for the number of CRF-positive mossy fiber terminals, there was no significant difference between RMN and the controls in the

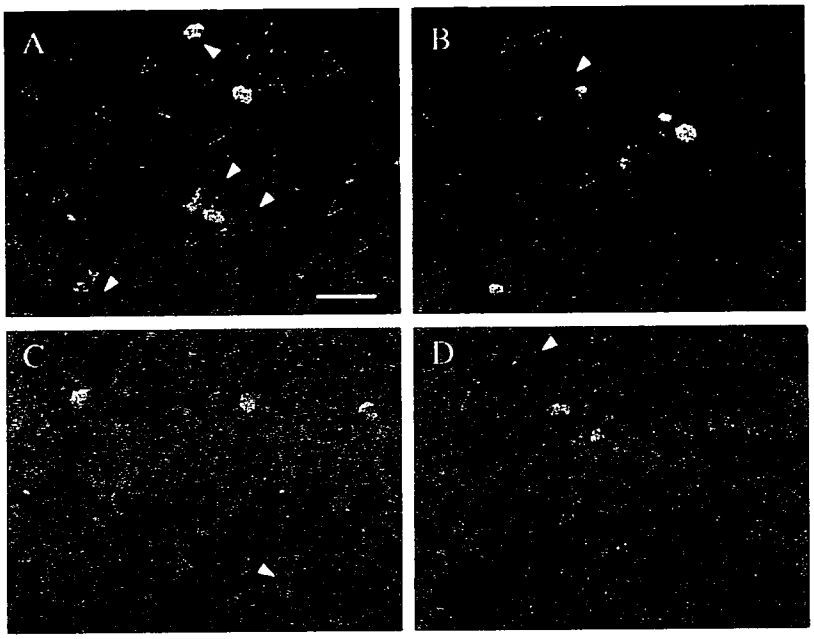

Fig. 2. Double immunofluorescence for calretinin (CR) and corticotropin-releasing factor (CRF) in coronal sections of vermal lobules X (A, B) and flocculus (C, D) of the cerebellum of a rolling mouse Nagoya (RMN) (A, C) and a control mouse (B, D). CR immunostaining appeared as green color (FITC), and CRF immunostaining appeared as red color (Cy3), respectively. CRF-positive mossy fiber terminals were much more in RMN than in controls, and some of those fibers were closely apposed to CR-positive UBCs. Open arrowheads indicate CRF-positive mossy fiber terminals. Closed arrowheads indicate CRF-positive mossy fiber terminals adjoining CR-positive UBCs. Scale bar = 20 μm.

number of those fiber terminals adjoining CR-positive UBCs in the flocculus (Table 3).

4. Discussion

The UBC is a class of glutamergic interneurons in the granule cell layer of vestibulocerebellum [7,8,12,13]. Electronmicroscopic studies demonstrate that the dendrites of UBCs make a synapse with mossy fiber terminals [8,13]. In the present study, a significantly greater number of CRF-positive mossy fiber terminals adjoining CR-positive UBCs were observed in the lobule X of RMN than that of controls. The fact that there was no difference in the number of CR-positive UBCs in the vestibulocerebellum suggests the increased number of CRF-positive mossy fiber terminals innervating CR-positive UBCs in the lobule X of RMN. CRF serves as a neuromodulator in the cerebellar circuits to increase glutamate sensitivity by decreasing afterhyperpolarization [2,3,10]. Therefore, CRF may facilitate CR-positive UBC-mediated excitatory pathways in the lobule X of RMN.

An intriguing result in the present study is that CRF-positive mossy fiber innervation of CR-positive UBCs was different among vestibulocerebellar lobules of RMN. The number of CRF-positive mossy fibers adjoining CR-positive UBCs was significantly greater in RMN than in controls in the lobule X but not in the flocculus. The lobule X receives otolith signals via mossy fibers from vestibular nuclei, reticular formation and lateral reticular nuclei and climbing fibers from the inferior olivary nucleus and plays a role in adaptation to otolith-mediated motion of the head [5]. Human patients with EA-2 impaired otolith-mediated linear vestibulo-ocular reflex but not semicircular-mediated angular vestibulo-ocular reflex [26]. Therefore, CRF may alter cerebellar adaptation for otolith-mediated linear motion of

Table 2
Number of corticotropin-releasing factor (CRF)-positive mossy fiber terminals per mm^2 of the granule cell layer in the vermal lobule X and flocculus of cerebellum (mean ± SEM)

Groups	n	Lobule X	Flocculus
RMN	8	491.3 ± 82.0*	154.7 ± 28.7
Control	8	189.6 ± 28.9	84.9 ± 27.2

Significant effects on group ($F_{1,28}$ = 18.67, P < 0.001), region ($F_{1,28}$ = 13.22, P < 0.002) and group × region interaction ($F_{1,28}$ = 5.15, P < 0.05) (two-way ANOVA).

* P < 0.001 vs. controls (contrast tests based on two-way ANOVA).

Table 3
Number of corticotropin-releasing factor (CRF)-positive mossy fiber terminals adjoining calretinin (CR)-positive UBCs per mm^2 of the granule cell layer in the vermal lobule X and flocculus of cerebellum (mean ± SEM)

Groups	n	Lobule X	Flocculus
RMN	8	77.4 ± 16.9*	15.9 ± 6.3
Control	8	13.3 ± 5.3	10.0 ± 6.9

Significant effects on group ($F_{1,28}$ = 9.16, P < 0.01), region ($F_{1,28}$ = 10.71, P < 0.005) and group × region interaction ($F_{1,28}$ = 7.14 P < 0.05).

* P < 0.001 vs. controls (contrast tests based on two-way ANOVA).

the head via CR-positive UBC-mediated excitatory pathways in the lobule X of RMN.

The presence of another UBC population in the mouse vestibulocerebellum, i.e., mGluR1α-positive UBCs, has been reported [14]. CR-positive and mGluR1α-positive UBC subsets are generated from distinctly different origins [24] and are supposed to organize non-overlapped different microcircuits in the cerebellum [14]. In the present study, the total number of CRF-positive mossy fiber terminals was significantly greater in the lobule X of RMN, possibly pointing to the enhanced CRF-positive mossy fiber innervation of granule cells or mGluR1α-positive UBCs. Further study will be necessary to examine CRF-positive mossy fiber innervation of mGluR1α-positive UBCs in the vestibulocerebellum of RMN.

In conclusion, the present study suggests an increased number of CRF-positive mossy fiber terminals innervating CR-positive UBCs in the lobule X but not in the flocculus of the RMN. Such regional differences in CRF-positive mossy fiber innervation of the RMN vestibulocerebellum seem to be correlated with specific clinical symptoms in human EA-2 patients [26]. These regional differences in neurochemical modulation of specific neuronal pathways in the cerebellum may well be the key to understanding the mechanisms of cerebellar ataxia development.

Acknowledgments

Mutant mice were kindly provided by Dr. S. Oda, Graduate School of Bio-Agricultural Science, Nagoya University. This study was supported by Grants-in-Aid for Scientific Research (15790940, 15591817 and 16700305) and Joint Research Project under the Japan–Korea Basic Scientific Cooperation Program from the Ministry of Education, Culture, Sports, Science and Technology, Japan.

References

[1] N.H. Barmack, R.W. Baughman, F.P. Eckenstein, Cholinergic innervation of the cerebellum of the rat by secondary vestibular afferents, Ann. N. Y. Acad. Sci. 656 (1992) 566–579.

[2] G.A. Bishop, Neuromodulatory effects of corticotropin releasing factor on cerebellar Purkinje cells: an in vivo study in the cat, Neuroscience 39 (1990) 251–257.

[3] G.A. Bishop, J.S. King, Differential modulation of Purkinje cell activity by enkephalin and corticotropin releasing factor, Neuropeptides 22 (1992) 167–174.

[4] E. Braak, H. Braak, The new monodendritic neuronal type within the adult human cerebellar granule cell layer shows calretinin-immunoreactivity, Neurosci. Lett. 154 (1993) 199–202.

[5] J.A. Buttner-Ennever, A review of otolith pathways to brainstem and cerebellum, Ann. N. Y. Acad. Sci. 871 (1999) 51–64.

[6] M.R. Diño, F.H. Willard, E. Mugnaini, Distribution of unipolar brush cells and other calretinin immunoreactive components in the mammalian cerebellar cortex, J. Neurocytol. 28 (1999) 99–123.

[7] M.R. Diño, M.G. Nunzi, R. Anelli, E. Mugnaini, Unipolar brush cells of the vestibulocerebellum: afferents and targets, Prog. Brain Res. 124 (2000) 123–137.

[8] M.R. Diño, R.J. Schuerger, Y.-B. Liu, N.T. Slater, E. Mugnaini, Unipolar brush cell: a potential feedforward excitatory interneuron of the cerebellum, Neuroscience 98 (2000) 625–636.

[9] C.F. Fletcher, C.M. Lutz, T.N. O'Sullivan, J.D. Shaughnessy Jr., R. Hawkes, W.N. Frankel, N.G. Copeland, N.A. Jenkins, Absence epilepsy in tottering mutant mice is associated with calcium channel defects, Cell 87 (1996) 607–617.

[10] E.A. Fox, D.L. Gruol, Corticotropin-releasing factor suppresses the afterhyperpolarization in cerebellar Purkinje neurons, Neurosci. Lett. 149 (1993) 103–107.

[11] Y. Mori, M. Wakamori, S. Oda, C.F. Fletcher, N. Sekiguchi, E. Mori, N.G. Copeland, N.A. Jenkins, K. Matsushita, Z. Matsuyama, K. Imoto, Reduced voltage sensitivity and activation of P/Q-type Ca^{2+} channels is associated with the ataxic mouse mutation *rolling Nagoya* (tg^{rol}), J. Neurosci. 20 (2000) 5654–5662.

[12] E. Mugnaini, A. Floris, The unipolar brush cell: a neglected neuron of the mammalian cerebellar cortex, J. Comp. Neurol. 339 (1994) 174–180.

[13] M.G. Nunzi, S. Birnstiel, B.J. Bhattacharyya, N.T. Slater, E. Mugnaini, Unipolar brush cells form a glutamatergic projection system within the mouse cerebellar cortex, J. Comp. Neurol. 434 (2001) 329–341.

[14] M.G. Nunzi, R. Shigemoto, E. Mugnaini, Differential expression of calretinin and metabotropic glutamate receptor mGluR1α defines subsets of unipolar brush cells in mouse cerebellum, J. Comp. Neurol. 451 (2002) 189–199.

[15] S. Oda, The observation of rolling mouse Nagoya (*rol*), a new neurological mutant, and its maintenance, Exp. Anim. 22 (1973) 281–286.

[16] S. Oda, A new allele of the tottering locus, rolling mouse Nagoya, on chromosome no. 8 in the mouse, Jpn. J. Genet. 56 (1981) 295–299.

[17] R.A. Ophoff, G.M. Terwindt, M.N. Vergouwe, R. van Eijk, P.J. Oefner, S.M.G. Hoffman, J.E. Lamerdin, H.W. Mohrenweiser, D.E. Bulman, M. Ferrari, J. Haan, D. Lindhout, G.-J.B. van Ommen, M.H. Hofker, M.D. Ferrari, R.R. Frants, Familial hemiplegic migraine and episodic ataxia type-2 are caused by mutations in the Ca^{2+} channel gene CACNL1A4, Cell 87 (1996) 543–552.

[18] K. Sawada, Y. Fukui, Expression of tyrosine hydroxylase in cerebellar Purkinje cells of ataxic mutant mice: its relation to the onset and/or development of ataxia, J. Med. Invest. 48 (2001) 5–10.

[19] K. Sawada, S. Komatsu, H. Haga, X.-Z. Sun, S. Hisano, Y. Fukui, Abnormal expression of tyrosine hydroxylase immunoreactivity in cerebellar cortex of ataxic mutant mice, Brain Res. 829 (1999) 107–112.

[20] K. Sawada, H. Haga, Y. Fukui, Ataxic mutant mice with defects in Ca^{2+} channel α_{1A} subunit gene: morphological and functional abnormalities in cerebellar cortical neurons, Congenit. Anom. Kyoto 40 (2000) 99–107.

[21] K. Sawada, H. Sakata-Haga, M. Ando, N. Takeda, Y. Fukui, An increased expression of Ca^{2+} channel α_{1A} subunit immunoreactivity in deep cerebellar neurons of rolling mouse Nagoya, Neurosci. Lett. 316 (2001) 87–90.

[22] K. Sawada, H. Sakata-Haga, S. Hisano, Y. Fukui, Topological relationship between corticotropin-releasing factor-immunoreactive cerebellar afferents and tyrosine hydroxylase-immunoreactive Purkinje cells in a hereditary ataxic mutant, rolling mouse Nagoya, Neuroscience 102 (2001) 925–935.

[23] K. Sawada, M. Ando, H. Sakata-Haga, X.-Z. Sun, Y.-G. Jeong, S. Hisano, N. Takeda, Y. Fukui, Abnormal expression of tyrosine hydroxylase not accompanied by phosphorylation at serine 40 in cerebellar Purkinje cells of ataxic mutant mice, rolling mouse Nagoya and dilute-lethal, Congenit. Anom. Kyoto 44 (2004) 46–50.

[24] G. Sekerková, E. Ilijic, E. Mugnaini, Time of origin of unipolar brush cells in the rat cerebellum as observed by prenatal bromodeoxyuridine labeling, Neuroscience 127 (2004) 845–858.
[25] Y. Tamaki, S. Oda, Y. Kameyama, Postnatal locomotion development in a neurological mutant of Rolling mouse Nagoya, Dev. Psychobiol. 19 (1986) 67–77.
[26] G. Wiest, J.R. Tian, R.W. Baloh, B.T. Crane, J.L. Demer, Otolith function in cerebellar ataxia due to mutations in the calcium channel gene CACNA1A, Brain 124 (2001) 2407–2416.
[27] T.A. Zwingman, P.E. Neumann, J.L. Noebels, K. Herrup, Rocker is new variant of the voltage-dependent calcium channel gene *Cacna1a*, J. Neurosci. 21 (2001) 1169–1178.

Otolaryngology–Head and Neck Surgery (2006) 135, 529-533

ORIGINAL RESEARCH

Natural history of benign paroxysmal positional vertigo and efficacy of Epley and Lempert maneuvers

Kazunori Sekine, MD, PhD, Takao Imai, MD, PhD, Go Sato, MD, Mahito Ito, MD, PhD, and **Noriaki Takeda, MD, PhD,** Tokushima and Osaka, Japan

We assessed the efficacy of Epley maneuver in patients with posterior canal benign paroxysmal positional vertigo (P-BPPV) and Lempert maneuver in patients with horizontal canal BPPV (H-BPPV). In patients with P-BPPV, positional vertigo in patients treated by Epley maneuver was significantly resolved more quickly than that in untreated patients. But in patients with H-BPPV, there were no significant differences of time course in remission of positional vertigo between untreated patients and patients treated by Lempert maneuver. Among the untreated patients, the positional vertigo in patients with H-BPPV was significantly resolved more quickly than that in patients with P-BPPV. Epley maneuver was effective for the treatment of patients with P-BPPV, whereas the efficacy of Lempert maneuver for the treatment of patients with H-BPPV was limited. The natural courses in remission of positional vertigo in untreated patients with H-BPPV showed significantly faster resolution than that in patients with P-BPPV.

Benign paroxysmal positional vertigo (BPPV) is a common vestibular disorder characterized by brief episodes of vertigo triggered by changes in head position. Most BPPV is caused by the lesion of the posterior semicircular canal (P-BPPV). But within recent years, many studies have reported another type of BPPV, in which the horizontal semicircular canal is affected (H-BPPV).[1-4] In case of P-BPPV, a geotropic torsional nystagmus is evoked when the patient is dropped back from the sitting position to a head hanging position with the head turned 45 degrees to the affected ear. On the other hand, in case of H-BPPV, a direction-changing geotropic horizontal nystagmus is evoked when the patient is rolled the head from side to side on supine position.

On the basis of canalithiasis hypothesis,[5,6] free-floating debris in the semicircular canal acts like a plunger and causes continuing movement of the endolymph even after head movement has ceased. This causes bending of the cupula to provoke positional nystagus and vertigo. Therefore, the canalith repositioning maneuver is the reasonable therapy for the treatment of BPPV. Nowadays, among canalith repositioning maneuvers, Epley maneuver for treatment of patients with P-BPPV[7] and Lempert maneuver for treatment of patients with H-BPPV[8] have become popular. There are some randomized control studies or a systematic review for the efficacy of Epley maneuver,[9-11] but not for the efficacy of Lempert maneuver.

In the present study, we assessed the efficacy of Epley maneuver and Lempert maneuver and time courses in remission of positional vertigo after the maneuvers were compared with natural history of remission in patients with P-BPPV and H-BPPV.

MATERIALS AND METHODS

Subjects

The present study included 127 patients with P-BPPV (54 male, 73 females, 13 to 82 years old; mean age, 60.1 ± 14.9 years) and 63 patients with H-BPPV (24 male, 39 females, 11-82 years old; mean age, 56.5 ± 16.1 years).

BPPV was diagnosed by the following criteria:

From the Department of Otolaryngology, University of Tokushima School of Medicine, Tokushima, Japan, (Drs Sekine, Sato and Takeda); Department of Otolaryngology and Sensory Organ Surgery, Osaka University Graduate School of Medicine, Osaka, Japan (Drs Imai and Ito).

This study was supported in part by a Health Science Research Grant for Specific Disease of the Ministry for Health and Welfare, Japan.

Reprint request: Kazunori Sekine, MD, PhD, Department of Otolaryngology, University of Tokushima School of Medicine, 3-18-15 Kuramoto, Tokushima 770-8503, Japan.

E-mail address: seky@pop21.odn.ne.jp.

0194-5998/$32.00 © 2006 American Academy of Otolaryngology–Head and Neck Surgery Foundation. All rights reserved.
doi:10.1016/j.otohns.2005.09.021

1. Absence of an identifiable central nervous system disorder able to explain the positional vertigo at neurological examination and neuroradiological studies of the brain.
2. No spontaneous nystagmus.
3. History of brief episodes of positional vertigo.
4. When the patients showed a direction-changing torsional positional nystagmus triggered by Dix-Hallpike maneuver, we diagnosed to P-BPPV, and when the patients showed a direction-changing geotropic horizontal positional nystagmus triggered by lateral head rotation on spine position, we diagnosed to H-BPPV.

We excluded the patients with symptoms that had lasted over 1 month before visiting hospital because the onset of their symptom was uncertain in the refractory cases.

Design

This study was a prospective clinical trial with patients randomized to the 2 treatment arms according to the treating institution where they originally sought medical care. In Tokushima University Hospital, 67 patients with P-BPPV were treated by modified Epley maneuver and 29 patients with H-BPPV were treated by Lempert maneuver every 2 weeks after the first visit to the hospital. In Kansai-Rosai Hospital, both 60 patients with P-BPPV and 34 patients with H-BPPV were untreated and asked to visit the hospital every 2 weeks (Table 1). After the patients were informed about canalith repositioning maneuver, the long-term effects of which were not evident based on previously reported meta-analysis,[12] informed consent of no treatment was obtained. In modified Epley maneuver,[13] the patient's head was turned 45 degrees toward to affected side in a sitting position. The patient was then moved from a sitting position into a head hanging position. After resolution of the nystagmus, the head was rotated to the opposite side. Next, the head and body were rotated 135 degrees from the supine position until the patient was facing down while lying in the supine position. Finally, the patient slowly sat up. In Lempert maneuver,[8] patient's head rotated 270 degrees to the unaffected side around the supine patient's longitudinal axis (barbecue rotation) (Fig 1). The rotation was performed in rapid steps of 90 degrees within a half second. Nystagmus induced by head movement was observed with an infrared CCD camera during both maneuvers. All patients were asked to come to the hospital every 2 weeks after the first visit. At every visit, they were interviewed and Dix-Hallpike maneuver was performed on each patient with P-BPPV and the lateral head rotation on spine position was performed on each patient with H-BPPV. After the absence of positional nystagmus was observed at any visit, they were asked when they felt that the positional vertigo has disappeared. Thus, the primary outcomes were self-reported onset and resolution of positional vertigo and time courses in remission of positional vertigo were then calculated.

This study was performed in accordance with the guidelines approved by the Committee for Medical Ethics of the University of Tokushima School of Medicine and an informed consent was obtained from each patient.

Statistical Analysis

Characteristics of untreated and treated patients were statistically analyzed with the Mann-Whitney U test, and values of $P < 0.05$ were considered significant. Residual rates of symptom were calculated after the first visit to our hospital with the Kaplan-Meier method. The differences between the 2 groups of patients in remission curves were analyzed using the log-rank test, and values of $P < 0.05$ were considered significant.

RESULTS

Characteristics of patients are listed in Table 1. Mann-Whitney U test showed no significant differences of age or sex between untreated patients and treated patients. And also, duration of symptom before visiting hospital had no significant difference between untreated patients and treated patients.

Fig 2 shows the residual rate of positional vertigo in untreated and modified Epley maneuver–treated patients

Table 1
Patient characteristics

		Treated patients			Untreated patients		
	Total	Total	P-BPPV	H-BPPV	Total	P-BPPV	H-BPPV
Sex							
Male (numbers)	78	39	30	9	39	24	15
Female (numbers)	112	57	37	20	55	36	19
Age							
Range (years)	11-82	13-82	13-82	25-79	11-83	17-83	11-82
Average ± SD (years)	58.9 ± 15.4	58.7 ± 15.5	59.6 ± 15.6	57.7 ± 14.4	59.1 ± 15.3	60.6 ± 14.3	56.4 ± 17.0
Duration of symptoms before visiting hospital							
Average ± SD (days)	6.4 ± 6.3	6.4 ± 6.3	6.9 ± 6.5	5.2 ± 5.9	5.2 ± 6.5	6.3 ± 7.6	3.4 ± 3.2
Totals	190	96	67	29	94	60	34

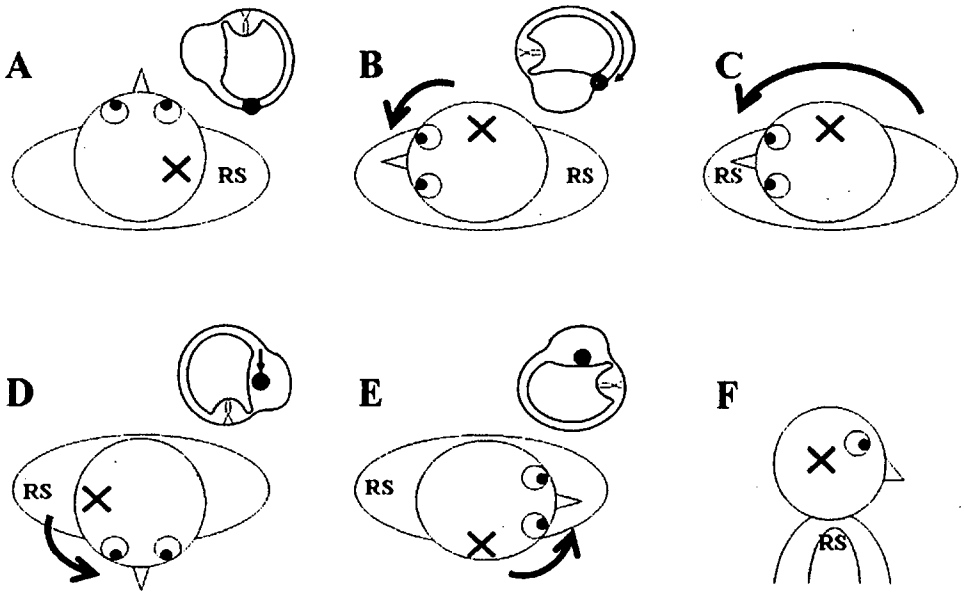

Figure 1 Lempert maneuver for treatment of H-BPPV. (**A**) Starting position: supine, (**B**) head rotation toward the unaffected side, (**C**), body turn from supine to prone while head position is maintained, (**D**) head rotation to nose-down position, (**E**) final head turn affected side to down position, (**F**) sitting up position. (*X* affected side; *RS*, right shoulder.)

with P-BPPV: 51.7% of untreated patients and 22.7% of treated patients at 1 week, and 20.0% of untreated patients and 9.7% of treated patients at 1 month. After modified Epley maneuver, the remission of the positional vertigo in patients with P-BPPV was significantly quicker than that in untreated patients with P-BPPV ($P = 0.003$). Fig 3 shows the residual rate of positional vertigo in untreated and Lempert maneuver–treated patients with H-BPPV. It was 30.9% of untreated patients 21.4% of treated patients at 1 week, and 7.1% of untreated patients and 5.4% of treated patients at 1 month. After Lempert maneuver, the positional vertigo in patients with H-BPPV disappeared with the same time course as that in untreated patients with H-BPPV ($P = 0.375$). Fig 4 shows the residual rate of positional vertigo in untreated patients with P-BPPV and with H-BPPV: 51.7% of P-BPPV and 30.9% of H-BPPV at 1 week, and 20.0% of P-BPPV and 7.1% of H-BPPV at 1 month. Among the untreated patients, the positional vertigo in patients with H-BPPV was significantly resolved more quickly than that in patients with P-BPPV ($P = 0.045$).

DISCUSSION

In the present study, positional vertigo in patients treated by modified Epley maneuver was significantly resolved more quickly than that in untreated patients. But in patients with H-BPPV, there were no significant differences of time course in remission of positional vertigo between untreated

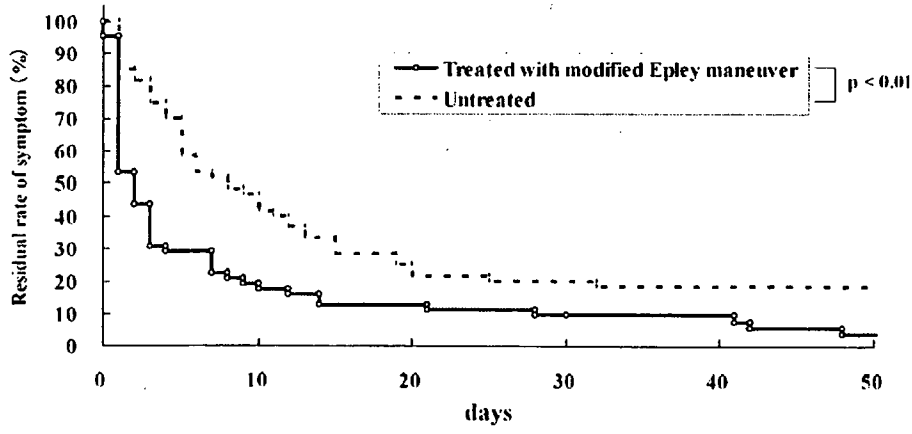

Figure 2 Residual rate of positional vertigo in patients with P-BPPV. (*Black line*, patients treated by modified Epley maneuver; *dotted line*, untreated patients.)

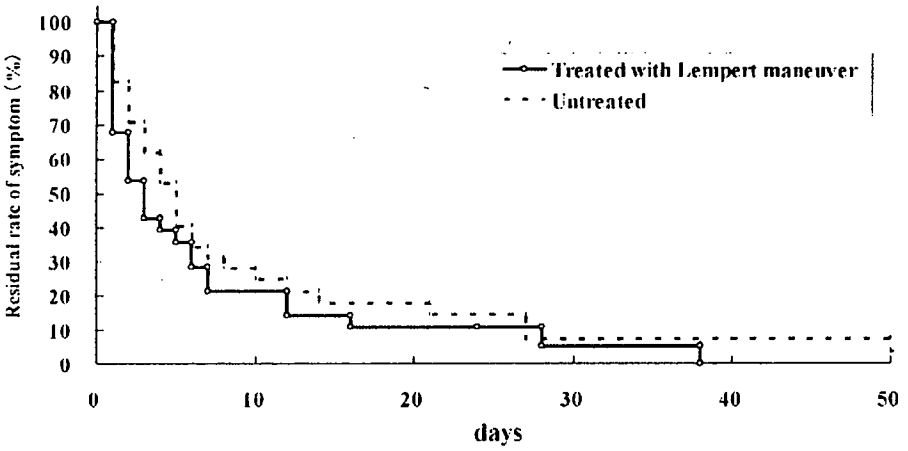

Figure 3 Residual rate of positional vertigo in patients with H-BPPV. (*Black line*, patients treated by Lempert maneuver; *dotted line*, untreated patients.)

patients and patients treated by Lempert maneuver. Among the untreated patients, the positional vertigo in patients with H-BPPV was significantly resolved more quickly than that in patients with P-BPPV.

There were some randomized control studies that show the efficacy of Epley maneuver.[9-11] A systematic review[12] said that the Epley maneuver is a safe, effective treatment for P-BPPV but shows no evidence of a long-term resolution of symptoms. In the present study, the Epley maneuver was effective within a month, but the efficacy was gradually decreased (Fig 2). The poor long-term efficacy of Epley maneuver can be explained by the high rate of spontaneous resolution of BPPV. In the present study, the residual rate of symptom of P-BPPV was 51.7% at 1 week and 20.0% at 1 month without treatment. Asawavichianginda et al[11] also showed after 3 months, 84% of patients with P-BPPV who received no treatment had converted to a negative Hallpike maneuver.

Although some studies reported the efficacy of Lempert maneuver for H-BPPV,[8] in the present study, there were no significant differences of the remission of positional vertigo between untreated patients and patients treated by Lempert maneuver (Fig 3). Consequently, we then compared with the natural courses in remission of positional vertigo in patients with P-BPPV and that in patients with H-BPPV. The spontaneous resolution rate of positional vertigo in patients with H-BPPV was significantly higher than that in patients with P-BPPV (Fig 4). Therefore, it is suggested that the efficacy of Lempert maneuver is overshadowed by such quick spontaneous remission of positional vertigo in patients with H-BPPV.

It can be explained by the orientations of the canals that the spontaneous remission of H-BPPV was shorter than that of P-BPPV. The long arm of the posterior semicircular canal hangs inferiorly from common crus. Therefore, any debris entering the canal essentially becomes trapped within and it is hard to get it out. In contrast, the lateral semicircular canal slopes slightly up and has its cupular at the upper end. Therefore, free-floating debris in the lateral canal would tend to float back out into the utricle as a result of natural head movements. In addition, repeated administration of the testing procedures for BPPV in the untreated patients may

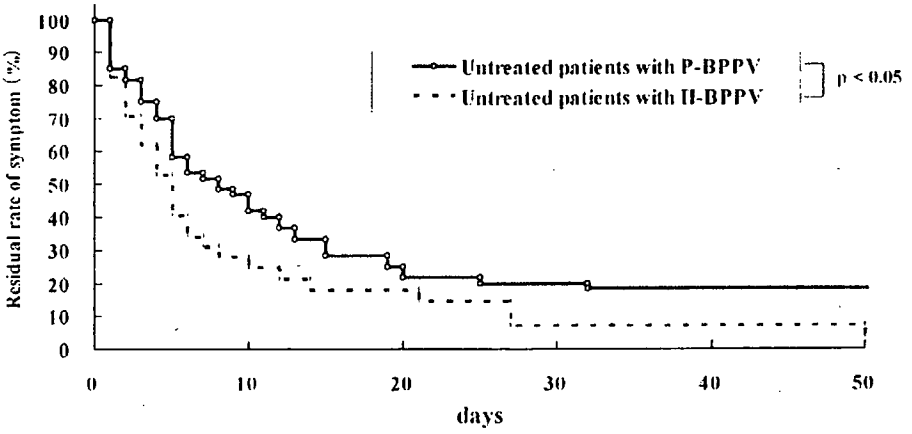

Figure 4 Residual rate of positional vertigo in untreated patients with P-BPPV and H-BPPV. (*Black line*, untreated patients with P-BPPV, *dotted line*, untreated patients with H-BPPV.)

actually have had some therapeutic effect that would potentially produce a remission rate that is greater than would be expected in truly untreated group, especially in patients with H-BPPV. And the patients in this study were very early in their disease process (Table 1), because of the criteria that excluded patients who had had symptoms for over 1 month before visiting hospital. This may account for the high spontaneous cure rate, especially in patients with H-BPPV. The therapeutic efficacy with both maneuvers may be different in refractory cases.

In this study, we assessed the efficacy of the Epley maneuver and the Lempert maneuver. The Epley maneuver was effective for the treatment of patients with P-BPPV, whereas the effects of Lempert maneuver for the treatment of patients with H-BPPV was limited. The natural course in remission of positional vertigo in untreated patients with H-BPPV was significantly quicker than that in untreated patients with P-BPPV.

REFERENCES

1. McClure JA. Horizontal canal BPV. J Otolaryngol 1985;14:30–5.
2. Baloh RW, Jacobson K, Honubia V. Horizontal semicircular canal variant of benign positional vertigo. Neurol 1993;43:2542–9.
3. Augusto PC, Giovanni V, Bruno F, et al. The treatment of horizontal canal positional vertigo: our experience in 66 cases. Laryngoscope 2002;112:172–8.
4. Dix MR, Hallpike CS. Pathology, systems and diagnosis of certain disorders of the vestibular system. Proc R Soc Med 1952;45:341–54.
5. Hall SF, Ruby RR, McClure JA. The mechanics of benign paroxysmal vertigo. J Otolaryngol 1979;8:151.
6. Parnes LS, McClure JA. Free floating endolymph particles: a new operative finding during posterior semicircular canal occlusion. Laryngoscope 1992;102:988–92.
7. Epley JM. New dimensional of benign paroxysmal positional vertigo. Otolaryngol Head Neck Surg 1980;88:599–605.
8. Lempert T, Ttiel-Wilck K. A positional maneuver for treatment of horizontal-canal benign positional vertigo. Laryngoscope 1996; 106:476–8.
9. Lynn S, Pool A, Rose D, et al. Randomized trial of the canalith repositioning procedure. Otolaryngol Head Neck Surg 1995;113:712–20.
10. Froehling DA, Bowen JM, Mohr DN, et al. The canalith repositioning procedure for the treatment of benign paroxysmal positional vertigo: a randomized controlled trial. Mayo Clinic Proc 2000;75:695–700.
11. Asawavichianginda S, Isipradit P, Snidvongs K, et al. Canalith repositioning for benign paroxysmal positional vertigo: a randomized, controlled trial. Ear Nose Throat J 2000;79:732–4,736–7.
12. Hilton M, Pinder D. The Epley (canalith repositioning) manoeuvre for benign paroxysmal positional vertigo. The Cochrane Library, Issue 3, 2003. Oxford: Update.
13. Harvey SA, Hain TC, Adamiec MS. Modified liberatory maneuver: effective treatment for benign paroxysmal positional vertigo. Laryngoscope 1994;104:1206–12.